

Simulation of polar stratospheric clouds: 2. Spectral aerosol extinction coefficient and PSC remote sensing possibilities

Ya.A. Virolainen, Yu.M. Timofeyev, A.V. Polyakov,
H. Steele,* K. Drdla,** and M. Newchurch***

Research Institute of Physics
at Saint Petersburg State University, Russia
* California State University, Northridge, USA
** NASA, USA
*** University of Alabama, Huntsville, USA

Received July 26, 2004

The spectral dependence of aerosol extinction coefficient (AEC) for several hundred of thousands of stratospheric aerosol and PSC realizations has been calculated based on Mie-theory algorithms. The means and covariance matrices for different scenarios of PSC transformation have been constructed. It has been shown that it is possible to use only 4 eigenvectors of AEC covariance matrices for approximation of AEC spectral dependence with 5% accuracy in 0.29 to 1.56 μm spectral region. The possibilities of retrieving the size distribution function (SDF) and its moment from AEC measurements with 5–25% accuracy have been studied. The regression method makes it possible to decrease essentially the relative *a priori* uncertainty of SDF of combined ensemble for the size range of 0.06–2 μm . This decrease is maximal for the 0.5–0.7- μm size particles (from 400 to 60%). Absolute *a priori* uncertainty of SDF decreases (from 3.5 to 0.35 cm^{-3}) in the size range of about 0.3 μm . In the range of the uncertainty curve maximum (0.1 μm), the absolute *a priori* uncertainty decreases from 7.6 to 3.8 cm^{-3} at the 5% AEC error, and to 5.5 cm^{-3} at 25%. Total cross-section area S is the best-determined value from all SDF moments. For combined ensemble, *a priori* uncertainty of S decreases by 4–5.5 times.

Introduction

Optical analysis of microstructure of aerosols and clouds is now widely used in ground-based and satellite experiments. Sunrise and sunset satellite measurements (eclipse technique) of the atmospheric transmission in the visible and IR spectral regions provide information on the spectral-altitude aerosol extinction coefficient (AEC) (SAGE-II, SAGE-III, Ozone-MIR, ROAM experiments and others^{1,10}). Solution of the inverse problem of the next level allows one to receive certain information on microstructure of the atmospheric aerosol and translucent clouds via AEC data.^{2–4}

On the base of the detailed PSC formation and dissipation model, 255 949 realizations of the size distribution function (SDF) were compiled and statistics of the SDF of PSC particles were studied.⁵ In this paper, statistics of the spectral extinction coefficient of the PSCs is considered as well as possibilities to its optimal parameterization and the regression approach to solving inverse problem on retrieval of the SDF of PSC particles from measured values of AEC.

1. Aerosol extinction coefficient of PSC and its optimal parameterization

As a first approximation, we supposed all PSC particles to be homogeneous spheres. AEC for different

PSC components (PSC under study includes particles of Liquid Aerosol, SAT Aerosol, NAT PSC, and Water Ice PSC fractions) and different scenarios of PSC formation⁵ was calculated based on the well known formula for polydisperse aerosols by Mie-theory algorithms for each wavelength and modeled SDF:

$$\sigma = N \int_0^{\infty} \pi r^2 Q(r, m) f(r) dr, \quad (1)$$

where $Q(r, m)$ is the extinction efficiency factor of an aerosol particle of the radius r and the complex refractive index m ; $f(r)$ is the SDF. The refractive index of sulfate solution particles (Liquid Aerosol) was taken from Ref. 8, at that, for three-component solutions, it was calculated based on averaged values for two-component solutions by the program described in Ref. 9. The refractive indices of other particles in the UV, visible, and near-IR spectral ranges were fixed as 1.40 for SAT Aerosol, 1.43 for NAT PSC, and 1.33 for Water Ice PSC fraction independent of wavelength and temperature. The imaginary part of the refractive index was set equal to zero in the ranges under study for all fractions. AEC were computed at 80 points (channels) of the spectral interval from 0.29 to 1.56 μm corresponding to SAGE-III satellite measurement range.¹¹

Figure 1 shows the mean values and the root-mean-square deviations (RMSD) of AEC for 4 PSC ensembles considered in Ref. 5.

Maximal AEC values are evidently observed for the ensemble IV. AEC variations are also strongest in this case, what is especially noticeable in the region from 0.29 to 1.03 μm . In the region of 0.3–0.5 μm , the mean AEC value slightly increases in the scenario IV and averages to 0.004 km^{-1} , while the RMSD increases in the 0.5 to 0.7 μm wavelength range (up to 0.004 km^{-1}). Then AEC decreases to 0.002 km^{-1} at the wavelength of 1.03 μm and down to 0.001 km^{-1} in the channels within the 1.52 to 1.56 μm wavelength range.

To all appearance, some anomalous AEC rise with the wavelength increase is due to predominance of larger particles of Liquid Aerosol fraction over smaller ones of other ensembles. Minimal AEC variations (about 0.001 km^{-1} independent of channel) are observed for the ensemble I. In this case spectral dependence of the mean AEC changes insignificantly; AEC varies from 0.002 in long-wave channels to 0.001 km^{-1} in short-wave ones.

Quite similar situation is observed with the ensemble III but with somewhat greater AEC RMSD values. In the ensemble II, mean values of the AEC vary from 0.002 to 0.0004 km^{-1} . Hence, the strongest relation between the mean values and RMSD of AEC is caused by the SDF shape (see Ref. 5) and this is observed for the scenarios II and IV.

Note, that the mean values and RMSD of AEC in the combined ensemble of realizations (SUM) are close in magnitude to similar values from the ensemble II, but with the less pronounced spectral dependence;

in SUM1 ensemble, where all the realizations belong to PSC (AEC values are more than 10^{-3} km^{-1} according to the selection criteria), these parameters are close to analogous of the model IV.

For all the observed models, covariance matrices of the spectral AEC D_{yy} , their eigenvectors, and eigenvalues were calculated as well as AEC optimal parameterization was constructed by the basis formed of eigenvectors of AEC covariance matrices (similar SDF parameterization was performed in Ref. 5).

Behavior analysis of 4 first eigenvectors for different PSC ensembles (Fig. 2) shows that the first eigenvector is practically similar for all the ensembles; the second one cuts zero line in the region of 0.63 μm in all the models except for the model III, where it happens in the region of 0.76 μm . The third eigenvector in the model I is opposite in phase with other models; the behavior of the fourth one is similar in the pairs of models I–III and II–IV. Four first eigenvectors of the AEC covariance matrix for the SUM and SUM1 ensembles differ little from each other. One can note that the eigenvectors of the combined ensemble practically coincide with those of the ensemble III.

Analysis of 6 first eigenvalues of AEC covariance matrix for different models shows already the second eigenvalue to be one order of magnitude less than the first one for all the models. The fourth eigenvalue for the models II and IV, the fifth for I, III, and the combined one are two orders of magnitude less than the first eigenvalue.

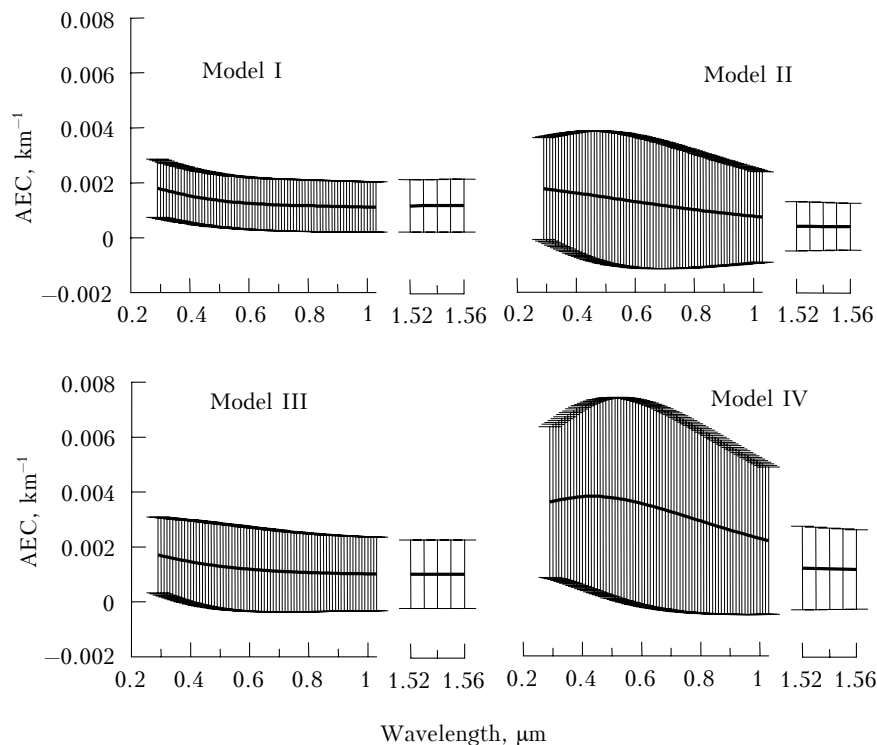


Fig. 1. Mean values and mean-square deviations of aerosol extinction coefficient in different ensembles of PSC realizations.

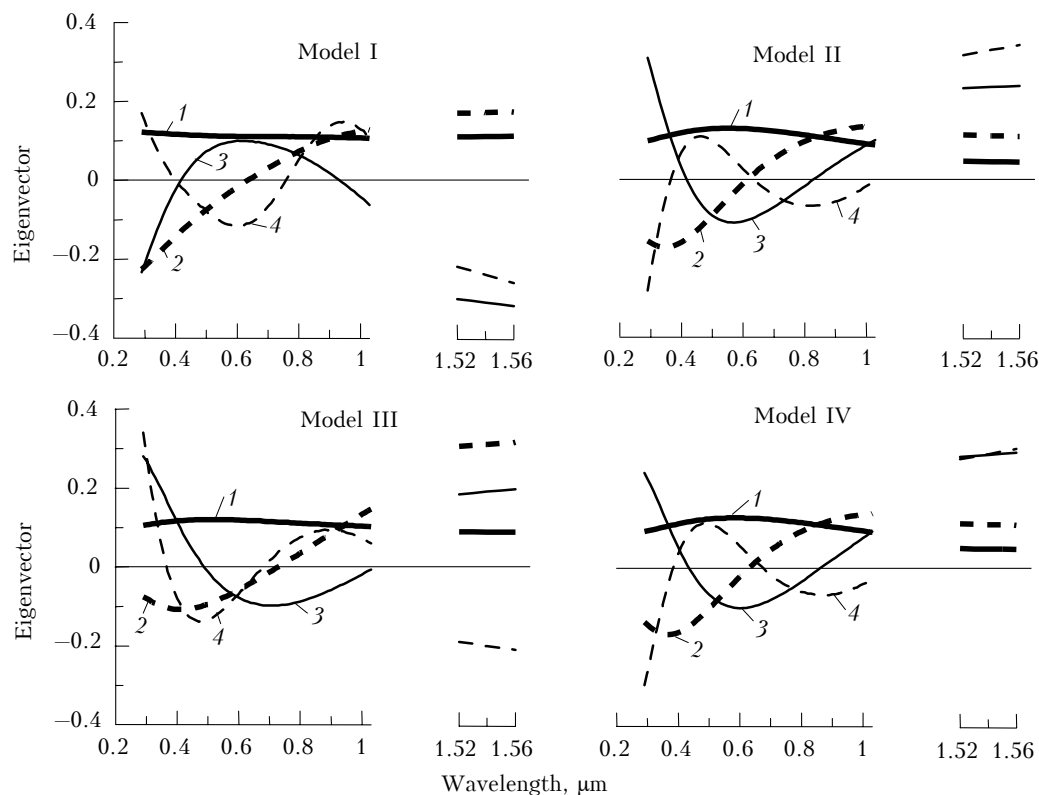


Fig. 2. Eigenvectors (1–4) of the AEC covariance matrix calculated by the PSC ensembles I–IV.

It is necessary to note, that in spite of different spectral dependences of eigenvectors for different models, it is quite sufficient to use only 4 vectors to achieve few-percent parameterization accuracy. It is evident from Fig. 3 showing the reduction of the relative error of the root-mean-square approximation with the increase of the number of eigenvectors.

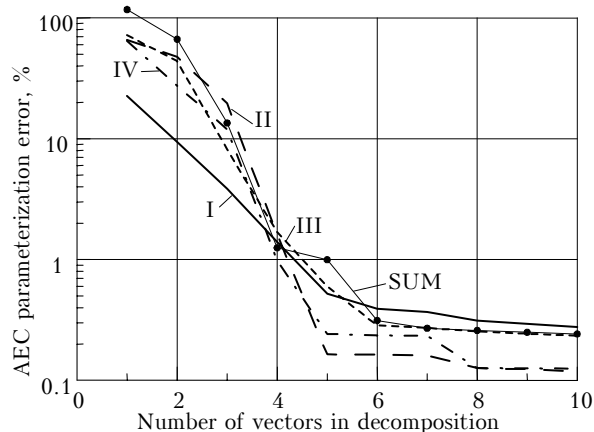


Fig. 3. Relative error of the AEC optimal parameterization in dependence on the number of vectors accounted for different PSC ensembles.

As is seen, the AEC approximation error decreases sharply at addition of eigenvectors (up to 5). The error is no more than 2% with 4 eigenvectors for all the ensembles. Figure 3 allows one to estimate information content, i.e., the number of independent

parameters gained from AEC measurements at varying accuracy. Thus, when AEC measurement accuracy is about 10%, one can gain 2 or 3 independent parameters for different PSC models, while at the accuracy of about 1%, 4 or 5 independent parameters can be retrieved. From the comparison of the optimal parameterization of SDF and AEC,⁵ one can note the parameterization of SDF to demand more eigenvectors than of AEC at a common required accuracy due to smoothing nature of the Mie-operator in calculating AEC of a polydisperse aerosol ensemble.

The spectral dependence analysis of the AEC parameterization relative error for the SUM ensemble with different number of eigenvectors accounted has shown spectral irregularity of the parameterization error if using only 3 first eigenvectors; in this case, the error varies within an order of magnitude depending on the spectral region. The error is no more than 3% if 4 vectors are used and the parameterization accuracy is somewhat lower in the long-wave channels. In summary of the analysis, it should be emphasized, that the parameterization error is no more than 5% with 4 first eigenvectors used for all the considered cases. Besides, the best parameterization accuracy is attained in the region from 1.52 to 1.56 μm for the ensemble I (better than 2%), in the short-wave channels (0.29–1.03 μm) for the ensembles II and IV although it strongly depends on spectrum (0.08–2%).

Also, the AEC parameterization has been carried out and its accuracy has been estimated for the cases of using a variety of “alien” vectors both for individual models and for the combined ensemble. For all the

models, use of 4 first vectors provides the AEC parameterization relative error no more than 5%. Hence, the analysis of the optimal AEC parameterization accuracy allows one to conclude that it is sufficient to use 4 first eigenvectors of the AEC covariance matrix for the SUM ensemble of PSC instead of AEC assignment in great number of spectral channels.

2. Regression method of the inverse problem solution relative to microphysical PSC characteristics

Let us now consider the possibility of applying the regression method to determination of the microphysical characteristics of a PSC from the AEC measurements. For implementation of the method, the cross-covariance matrix has been calculated characterizing the steady-state correlations between aerosol extinction coefficients and aerosol and PSC microphysical characteristics. The AEC and SDF cross-covariance matrices relate the quantities by the regression equation

$$x = x_a + D_{xy}(D_{yy} + I\epsilon^2)^{-1}(y - y_a), \quad (2)$$

where x is the SDF (and its moments); y is the AEC; D relates to corresponding blocks of the united cross-covariance matrix; I is the unity matrix; ϵ is the AEC measurement error. Subscript "a" corresponds to the average ensemble value.

At the first stage of solving the regression problem on determination of SDF and its moments, we supposed AEC to be known within 5–25% accuracy (e.g., from satellite SAGE-III measurements). So, for each of the PSC model, microphysical characteristics (SDF and its moments) were determined from Eq. (2) based on the above covariance matrices D_{yy} and D_{xy} with regard for AEC measurement error for each PSC realization; then root mean-square characteristics of retrieval accuracy of the SDF parameters were calculated.

The relative accuracy analysis of the regression for the PSC models I–IV has shown the maximal decrease of *a priori* uncertainty for the model I to be in the size ranges of 0.06–0.2 and 1–3 μm while for other models – in the range of 0.1–1 μm . The most informative AEC values with respect to SDF are observed for the scenarios II and IV, where *a priori* SDF uncertainty can decrease by one order of magnitude (from 100–200 to 10–15%) in some size range.

The analysis of absolute regression errors has shown 2 peaks of *a priori* uncertainty for PSC formation scenarios II and IV in contrast to the other scenarios. In addition to the main peak (for the particles of about 0.1 μm in size), the SDF variability maximum is observed for the particles of 0.2–0.3 μm size. In the same size range, the maximum information content of the AEC measurements with respect to SDF (absolute *a priori* uncertainty decreases by one order of magnitude) is observed as well. There is no

such effect in other models. Judging by the variability of the number of particles ($4\text{--}6\text{ m}^{-3}$), it belongs to the Liquid Aerosol fraction. In the region of main maximum of the variability for all the models, a 1.5-fold decrease (model III) and 3-fold decrease (model I) of *a priori* uncertainty are observed.

When we interpret AEC measurements in reality, we do not know, which model can be assigned to a particular realization. In this connection, the possibility of solving the inverse problem for the combined PSC ensemble is of principle interest from the practical point of view.

Figure 4 shows both relative and absolute estimation of error of SDF retrieval from AEC measurements for the combined PSC ensemble. The relative *a priori* uncertainty and corresponding regression errors at 5 and 25% AEC accuracy are shown in Fig. 4a, Fig. 4b shows similar absolute characteristics.

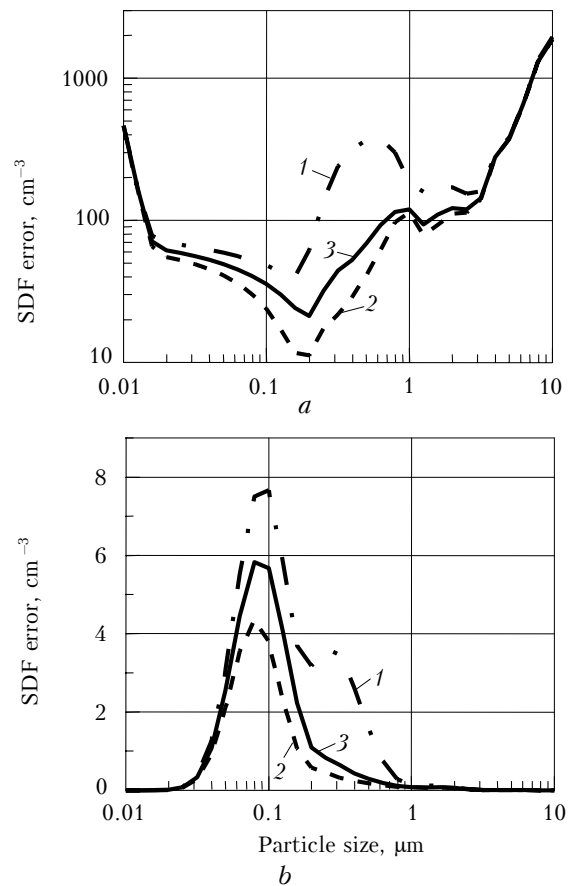


Fig. 4. Relative (a) and absolute (b) errors of SDF regression from AEC with 5 and 25% accuracy in the PSC combined ensemble SUM; *a priori* (1); 5% AEC accuracy (2); and 25% AEC accuracy (3).

From the comparison of results on the combined ensemble with other particular ensembles, we can note that the model I better fits the estimations obtained for fine particles (less than 0.2 μm), while the other models – in the region of larger particles. On the whole, the essential decrease of relative *a priori* SDF

Error of determination, σ , and *a priori* variability (%) of different SDF moments in PSC retrieved from AEC values measured with 5 and 25% accuracy for different PSC models

Parameter	σ_{AEC} , %	I	II	III	IV	SUM
<i>N</i>	<i>A priori</i>	38	37	38	28	38
	σ 5	12.7	22.2	20.7	18.2	20.9
	σ 25	21.5	30.7	29.3	24.3	30.1
<i>S</i>	<i>A priori</i>	62	108	73	83	85
	σ 5	3.6	8.5	21.1	6.3	15.4
	σ 25	10.0	14.8	26.1	11.3	21.0
<i>V</i>	<i>A priori</i>	121	260	174	241	174
	σ 5	70	115	128	109	127
	σ 25	72	184	133	158	130

uncertainty is observed for the size range of 0.06–2 μm , and the decrease amounts to about one order of magnitude for particular size ranges (e.g., from 400 to 60% for the particles of 0.5–0.7 μm in size).

As is seen from Fig. 4b, the absolute *a priori* uncertainty curve has an additional maximum at sizes about 0.3 μm . The maximal decrease of absolute *a priori* uncertainty of aerosol particles concentration (from 3.5 to 0.35 cm^{-3}) falls at the same size range.

Within the region of the main peak of the uncertainty curve (0.1 μm), the absolute decrease occurs from 7.6 to 3.8 cm^{-3} at 5% AEC error and down to 5.5 cm^{-3} at the 25% AEC error. It is necessary to note, that the order of *a priori* SDF uncertainty is the same for SUM1 ensemble, but *a priori* uncertainty values are almost two times less.

Besides, it is interesting to analyze, what integral characteristics of SDF⁵ can be retrieved from AEC measurements. The table presents *a priori* variability and the regression error for 3 first SDF moments (the total number *N*, total area *S*, and the total volume *V* of all aerosol particles), which can be obtained at 5 and 25% AEC errors in 80 channels of the spectral interval of 0.29–1.56 μm (SAGE-III satellite measurement range).

The results given refer to PSC ensembles I–IV and the combined one. As is seen, the total area *S* is the best-determined parameter. *A priori* variability diminishes by the factor of 3.5–17 (from 62–108 to 3.6–21%) at 5% AEC accuracy and by the factor of 3–7.5 (down to 11.3–26%) at 25% AEC accuracy. The worst retrieval accuracy of *S* is observed for the ensemble III, which affects significantly estimation of the combined ensemble of PSC realizations.

It is evident from the table, that *a priori* uncertainty of *S* decreases 5.5-fold (from 85 to 15%) at 5% AEC accuracy and 4-fold (down to 21%) at 25% AEC accuracy for the case of the combined ensemble, which is of great practical interest. Analyzing the relative regression accuracy of other SDF moments, one can note the 2-fold decrease of the relative *a priori* uncertainty at 5% AEC accuracy for the total number of particles (in the combined ensemble it is from 38 to 21%). The regression accuracy is significantly low at 25% AEC accuracy (on the average, the error is one third as low as *a priori* uncertainty; the error is equal to 30% for the combined ensemble).

The best estimations of *N* are observed for the model I (3- and 2-fold decrease of *a priori* uncertainty at 5 and 25% AEC error, respectively). As regards the higher SDF moments of aerosol particles, an insignificant decrease of *a priori* uncertainty of their total volume from 174 to 127–130% is observed (depending on the AEC error).

As for *V*, the increase of AEC measurement accuracy results in an increase of the regression accuracy only for PSC formation scenarios II and IV, while for other scenarios and the combined model it does not improve the regression estimation of the SDF moments. The regression accuracy for SUM1 ensemble is somewhat worse as compared with the SUM because of lower correlations between AEC and SDF and its moments due to abandonment of PSC realizations with lower AEC values, e.g. due to reduction of AEC measurement information content.

Conclusion

The spectral PSC aerosol extinction coefficient (AEC) for a great number of atmospheric aerosol realizations has been calculated based on Mie-theory algorithms. Optical statistics of AEC have been analyzed. It has been shown that it is sufficient to use only 4 eigenvectors for the optimal AEC parameterization in 0.29–1.56 μm spectral region (SAGE-III spectral range) to approximate AEC spectral dependence. The possibilities of applying the multiregression method to retrieve the size distribution function and its moments from AEC measurements with 5–25% accuracy have been studied. Total surface area *S* has been shown to be the best-determined value among all the SDF moments. In this case, *a priori* uncertainty of *S* decreases 4 to 5.5 times. As for total number of aerosol particles, only half decrease of *a priori* uncertainty is possible; for total volume *a priori* uncertainty decrease is insignificant.

Acknowledgments

This work is financially supported by St. Petersburg Administration (Grant PD03–1.5–114), National Aeronautics and Space Administration (Grant NAG 5–11248), Russian Foundation for Basic Research (Grant 03–05–64626), and Universities of Russia (Grant UR.01.01.044).

References

1. A.V. Polyakov, Yu.M. Timofeyev, A.V. Poberovskii, A.V. Vasiliev, *Izv. Ros. Akad. Nauk, Fiz. Atmos. Okeana* **37**, No. 2, 213–222 (2001).
2. J. Lenoble and P. Pruvost, *J. Climate Appl. Meteorol.* **22**, No. 10, 1717–1725 (1983).
3. L.W. Thomason, *J. Geophys. Res. D* **96**, No. 12, 22501–22508 (1991).
4. H.M. Steele and R.P. Turco, *J. Geophys. Res. D* **102**, No. 14, 16737–16747 (1997).
5. Ya.A. Virolainen, Yu.M. Timofeyev, A.V. Polyakov, H. Steele, K. Drdla, and M. Newchurch, *Atmos. Oceanic Opt.* **18**, No. 3, 264–269 (2005).
6. K. Drdla, “*Applications of a model of polar stratospheric clouds and heterogeneous chemistry*,” Ph. D. Thesis, UCLA (1996).
7. K. Drdla, M.R. Shoeberl, and E.V. Browell, *J. Geophys. Res. D* **108**, No. 5, 8312 (2003).
8. H.M. Steele and P. Hamill, *J. Aerosol Sci.*, No. 12, 517–528 (1981).
9. B. Luo, U.K. Krieger, and T. Peter, *Geophys. Res. Lett.* **23**, 3707–3710 (1996).
10. G.K. Yue, *J. Geophys. Res. D* **105**, No. 11, 14719–14736 (2000).
11. SAGE III ATBD Team, SAGE III Algorithm Theoretical Basis Document (ATBD) Transmission Level 1B Products LaRC 475–00-108 version 2.1 26 March 2002 (the report can be read at the site www-sage3.larc.nasa.gov), 52 pp.